AN ELECTROHYDRODYNAMICALLY INDUCED SPATIALLY PERIODIC CELLULAR STOKES-FLOW

C.V. Smith, Jr. and J. R. Melcher

NsG 368 CSR-TR-67-4 May 1967

AN ELECTROHYDRODYNAMICALLY INDUCED SPATIALLY PERIODIC CELLULAR STOKES-FLOW

C. V. Smith, Jr., and J. R. Melcher

Department of Electrical Engineering
Massachusetts Institute of Technology

Summary

An experiment is described in which a spatially periodic, time-invariant electric field is used to create a spatially periodic cellular flow by the action of an electric shear stress in the region of a fluid-fluid interface. The cellular motion is closely related to large-amplitude interfacial deformations observed when an electric field stresses the interface between two fluids having nearly the same electrical conductivity. A simple theoretical model is developed for the cell streamlines, flow velocity, and distribution of electric potential, and this model is shown to be in agreement with the experimental observations.

AN ELECTROHYDRODYNAMICALLY INDUCED SPATIALLY PERIODIC CELLULAR STOKES-FLOW

C. V. Smith, Jr., and J. R. Melcher

Department of Electrical Engineering
Massachusetts Institute of Technology

I. Introduction

There have been a number of investigations concerned with the instability of a fluid-fluid interface in the presence of electric fields.[1-4] For the majority of this work, attention is limited to small-amplitude interfacial deformations, as is appropriate in predicting the onset of instability. Under certain conditions, large-scale deformations of an electrically stressed interface have been observed to be dynamically stable. With a constant-amplitude electric field imposed perpendicular to an initially planar interface, the shape and position of these deformations are nearly stationary. Qualitatively, one can distinguish between at least two deformation types. If the imposed field is alternating at a sufficiently high frequency that the interface cannot respond parametrically and supports a negligible free surface charge, the interface deforms into an array of stationary spikes with rounded tips. In this case the fluid, as well as the interface, appears to be static. In consequence of the fact that the polarization force acting in this situation is everywhere normal to the interface, the bulk of the fluid is also static.[5]

Figure 1 shows a second type of deformation found when the interface between acetophenone and glycerin is stressed by an electric field. In general, the size of these deformations is also

proportional to the intensity of the applied field. However, the fluid deformations in this case are not quite stationary. The situation appears very much like a congregation of seals with smoothly rounded heads pointed skyward. As the "seals" socialize, the heads move gently up and down, and sway back and forth.[6] Careful examination shows that the fluids above and below the interface are in motion. There is no clear threshold for the appearance of the deformations as the electric field is raised.

The mechanism for this "quasi" stationary state is believed to be closely related to the existence of interfacial electrical shearing tractions that give rise to cellular convection in the bulk of the fluid adjacent to the deformed interface. These shear tractions are possible because the fluids conduct electrically to approximately the same degree. The cellular convection is consistent with the work of Taylor, McEwan, and DeJong[7] who have observed cells in and around a spherical drop of fluid stressed by an applied electric field.

It is recognized at the outset that the large-amplitude equilibria are made possible by nonuniformities in the electric field. Much of the complication in providing a theoretical picture of the phenomena arises because these nonuniformities are brought about by the deformations themselves. In the work presented here, cellular convection is studied by deliberately imposing a nonuniformity in the electric field. An experiment is described in which a spatially periodic, time-invariant electric field is used to create a spatially periodic cellular flow by the action of an electric stress in the region of a fluid-fluid interface. The experiment is arranged in such a way as to allow the establishment of this flow without significant deformation of the interface. The self-consistent effects of interface distortion needed to understand fully the equilibria shown in Fig. 1 represent a further complication that will not be developed here.

The geometry of the model is shown in Figure 2. There are two slightly-conducting fluids above a segmented electrode along which is impressed a sinusoidally-distributed, time-independent electrical potential $V_o \cos(\pi x/\ell)$. The fluid-fluid interface is considered to remain parallel to and at a fixed distance above the conducting electrode. The region above the interface extends to infinity, and gravity is taken as acting in the minus y direction. The parameters and variables are to be denoted either by a subscript or superscript a or b; a indicating variables associated with the region above the interface, and b those in the region below. Finally, the flow considered is restricted to be two-dimensional - that is, no variation in the z-direction. The cells produced in this case are of the simplest type realizable, and are called by Chandrasekhar "roll cells".[8]

There are two essential aspects, namely: one of the fluids is in electrical contact with the electrodes used to establish the electric field, and the charge relaxation process dominates charge convection. The first condition prevents induced charge from forming at the fluid-fluid interface in such a way as to eliminate the shear stress of electrical origin; the second condition implies that the electric field is not dependent on the fluid motion. This in turn implies that the electric field is essentially determined only by the electrode structure, fluid-fluid interface geometry, and the electrical properties of the fluids. Under these conditions, the applied electric field creates a shear stress at the fluid-fluid interface which induces the fluid motion, and an equilibrium flow is established when the electrical stress is balanced by the viscous stress arising from this fluid motion.

II. Theoretical Model: Equations and Boundary Conditions

Because the fluids are assumed to be slightly-conducting, there are no large currents which could produce significant magnetic fields. Therefore, the magnetic field will be assumed negligible and the

electric field $\bar{E}$ satisfies the equations

$$\nabla \times \bar{E} = 0 \tag{1}$$

and

$$\nabla \cdot \varepsilon\bar{E} = q \tag{2}$$

where q is the free charge density and ε is the permittivity. Conservation of free charge requires

$$\nabla \cdot \bar{J} + \partial q/\partial t = 0 \tag{3}$$

where $\bar{J}$ is the free current density. For an observer at rest relative to a material particle, Ohm's law in the form $\bar{J}' = \sigma\bar{E}'$ is assumed to be valid (the primes indicate variables in the local fluid reference frame and σ is the conductivity). This constituent law expressed in the laboratory is

$$\bar{J} = \sigma\bar{E} + q\bar{v} \tag{4}$$

where $\bar{v}$ is the velocity of the fluid.[9]

The physical laws which govern the motion are conservation of mass

$$\nabla \cdot \rho\bar{v} + \partial\rho/\partial t = 0 \tag{5}$$

and conservation of momentum in the form

$$\rho\frac{D\bar{v}}{Dt} = -\nabla(p + \rho gy) + \mu\nabla^2\bar{v} + \bar{f}^{(e)} \tag{6}$$

where ρ is the mass demsity, p is the hydrodynamic pressure, g is the magnitude of the acceleration due to gravity, μ is the fluid viscosity (considered constant), $\bar{f}^{(e)}$ is the force density of electrical origin, and $\frac{D}{Dt} \equiv \frac{\partial}{\partial t} + \bar{v} \cdot \nabla$. For a fluid, the form of the force of electrical origin is given by

$$\bar{f}^{(e)} = q\bar{E} - \frac{1}{2}\bar{E}\cdot\bar{E}\nabla\varepsilon + \nabla\left[\frac{1}{2}\rho\left(\frac{\partial\varepsilon}{\partial\rho}\right)_T \bar{E}\cdot\bar{E}\right] \tag{7}$$

where the subscript T indicates an isothermal process. The derivation of this force density is carried out in detail in the various texts.[10]

An initial simplification of this model may be made by consideration of how charge relaxation behaves in the presence of charge convection; equations (2) - (5) may be combined to obtain

$$\frac{D}{Dt}\left(q/\rho\right) + \frac{\sigma}{\varepsilon}\left(q/\rho\right) = 0 \qquad (8)$$

For every fluid particle, the charge relaxation mechanism operates in spite of the presence of charge convection to force the quantity q/ρ to relax to zero as $\exp-(\sigma/\varepsilon)t$. The free charge must vanish in the interior independently of the fluid motion. The convection process may alter the charge distribution in space, but cannot change the relaxation time ε/σ associated with the relaxation of the free charge density.

With q equal to zero in the bulk of the fluids, the two bulk coupling terms $q\bar{v}$ and $q\bar{E}$ in equations (4) and (6) are zero; therefore the field and fluid must couple in the interface region as specified by the necessary boundary conditions. One further simplification may be effected by incorporating the electrostriction term of equation (7) into the pressure term of the equation of motion (6), by defining an effective pressure π such that

$$\pi = p + \rho g y - \frac{1}{2}\rho\left(\frac{\partial \varepsilon}{\partial \rho}\right)_T \bar{E}\cdot\bar{E} \qquad (9)$$

Examination of the bulk equations reveals that there are 12 boundary conditions, four for the electric field and eight for the velocity. The condition that the electric field and velocity must vanish as $y \to \infty$ provides one of the four electric field conditions and two of the eight fluid conditions; hence the remaining nine conditions must be obtained at the interface and the conducting electrode. The model requires the normal and shear velocities at

the electrode be zero and the normal velocities at the interface to be zero. For the electric field, the tangential component is required to be continuous at the interface, and the normal component of current in the fluid must satisfy continuity at the interface. In addition, the field must match the potential applied to the electrode. The preceding comprises seven conditions; continuity of tangential velocity and the total shear stress at the interface are the remaining conditions. Of the boundary conditions, the two which provide the coupling mechanisms are of the greatest interest, namely: conservation of charge and continuity of the total shear stress at the interface. The condition for conservation of charge is written in the form [11]

$$\bar{n}\cdot(\bar{J}^a - \bar{J}^b) + \nabla_\Sigma \cdot Q\bar{v} + {}^{\partial Q}/_{\partial t} = 0 \qquad (10)$$

where Q is the surface charge density, $\bar{n}$ is the unit normal for the interface directed from region b to region a and $\nabla_\Sigma \cdot Q\bar{v}$ is the surface divergence of surface current density $Q\bar{v}$. It is assumed that the fluid properties in the region of the fluid-fluid interface are the same as those for fluid in the bulk, and hence there is no surface current due to a conduction mechanism (i.e., due to the presence of a surface conductivity). It therefore follows that the only surface currents allowed in this model occur as convection of free surface charges. The condition on the total shear stress may be obtained from a stress tensor representation of the right-hand side of equation (6), as follows:

$$\bar{f}_{total} = \nabla \cdot \bar{\bar{T}} \qquad (11)$$

where

$$\bar{\bar{T}} = -(\pi + \frac{1}{2}\bar{E}\cdot\bar{E})\,\bar{\bar{I}} + \mu(\nabla\bar{v} + \bar{v}\nabla) + \varepsilon\bar{E}\,\bar{E} \qquad (12)$$

and $\overline{\overline{I}}$ is the unit tensor of second order. The vector traction acting on an element of the fluid-fluid interface is

$$\bar{\tau} = (\overline{\overline{T}}^a - \overline{\overline{T}}^b) \cdot \bar{n} \tag{13}$$

Letting the subscript s denote the tangential direction, the condition on the total shear stress is

$$\mu_a \left(\frac{\partial v_n^a}{\partial x_s} + \frac{\partial v_s^a}{\partial x_n} \right) - \mu_b \left(\frac{\partial v_n^b}{\partial x_s} + \frac{\partial v_s^b}{\partial x_n} \right) = - \varepsilon_a E_s^a E_n^a + \varepsilon_b E_s^b E_n^b \tag{14}$$

where x_s and x_n are variables in the normal and shear directions respectively. Recalling that v_n is zero along the interface, this reduces to

$$\mu_a \frac{\partial v_x^a}{\partial y} - \mu_b \frac{\partial v_x^b}{\partial y} = - \varepsilon_a E_x^a E_y^a + \varepsilon_b E_x^b E_y^b \tag{15}$$

In those cases for which the convection of charge may be neglected (second term in Eq. 10), the field is completely uncoupled from the fluid motion and is determined only by the electrode potential and fluid-fluid interface geometry. This means the problem separates under these conditions into two parts: first, the solution of a linear field problem, and second, determination of the fluid flow produced by the imposed electric field. The field induces this flow through the action of the electric shear stress at the fluid-fluid interface, as given by Equation (15). Expressing the equations for the model in non-dimensional form secures three-dimensionless parameters; the ordinary Reynolds' number

$$Ry = \frac{\rho u \ell}{\mu} \tag{16}$$

which is a measure of the importance of the convective inertial term relative to the viscous term $\mu \nabla^2 \bar{v}$, the electric Reynolds' number [12]

$$Re = \frac{\varepsilon u}{\sigma \ell} \tag{17}$$

which is a measure of the importance of the charge convection relative to charge conduction, and the interaction parameter

$$S = \frac{\mu \ell u}{\varepsilon v^2} \tag{18}$$

which is a measure of the electromechanical energy conversion. The quantities u, ℓ, and v are respectively the characteristic velocity, length, and electric potential. From Buckingham's π-theorem[13] there exists a functional relation between these parameters, say

$$S = S\,(Re, Ry) \tag{19}$$

This indicates for the special case that Re and Ry approach zero, S becomes a constant, and the velocity must be proportional to the square of the applied potential. In the experiment associated with this model, interest was confined to an investigation of the steady state corresponding to this limiting case. Therefore, in the following analytical solution, steady state is assumed and the two terms, $\rho\bar{v} \cdot \nabla\bar{v}$ and $\nabla_{\Sigma} \cdot Q\bar{v}$, are neglected. This allows the separation of the problem as indicated. The range of validity of this solution is given in terms of the Reynolds' numbers as $Re < 1$ and $Ry < 1$.

III. Solution for the Case Re < 1 and Ry < 1

With the field uncoupled from fluid motion, a scalar potential is used to facilitate the field solution. Defining the potential such that $\bar{E} = -\nabla \phi$ and recalling that $q = 0$, Eqs. (1) and (2) indicate ϕ must satisfy Laplace's equation,

$$\nabla^2 \phi = 0 \tag{20}$$

in each of the fluid regions. The solutions matching the boundary conditions are

$$\phi^a = \frac{\ell E_o}{\pi} e^{\frac{-\pi y}{\ell}} \cos(\pi x/\ell) \tag{21}$$

and

$$\phi^b = \frac{\ell E_o}{\pi} \left[\cosh(\pi y/\ell) - \frac{\sigma_a}{\sigma_b} \sinh(\pi y/\ell)\right] \cos(\pi x/\ell) \tag{22}$$

where

$$E_o = \frac{\pi V_o}{\ell} \left[\cosh(\pi d/\ell) + \frac{\sigma_a}{\sigma_b} \sinh(\pi d/\ell)\right]^{-1}$$

The electric field, given by $-\nabla\phi$, is as shown in Fig. 3.

The field induces the flow by the action of the electrical shear stress at the interface. The electric shear stress (which is proportional to $E_x E_y$) must have a periodic variation in the x-direction with a period which is half the period of the field variation. The spatial period of the flow should be half that of the field. As with the field equations, it is convenient to solve for the fluid motion using an auxiliary function. Hence,

$$\bar{v}(x,y,t) = \bar{i}_x \left[\frac{\partial \psi}{\partial y}\right] - \bar{i}_y \left[\frac{\partial \psi}{\partial x}\right] \tag{23}$$

where ψ is the z component of the vector stream function.[14] This satisfies conservation of mass.

Substitution of Eq. (23) into the curl of Eq. (6) -- with $\rho\bar{v}\cdot\nabla v$ omitted -- yields

$$\nabla^2\nabla^2\psi = 0 \tag{24}$$

the biharmonic equation.

The restriction to a flow which is periodic in the x-direction suggests a solution of the form

$$\psi = f(y)\ \sin(2\pi x/\ell) \tag{25}$$

The function f(y) must satisfy the equation

$$\left[\frac{d^2}{dy^2} - (2\pi/\ell)^2\right]^2 f(y) = 0 \tag{26}$$

and choosing solutions which satisfy the boundary conditions at infinity obtains, for the upper fluid,

$$f^a = U(c_1^a + c_2^a\, y)e^{-2\pi y/\ell} \tag{27}$$

and, in the lower fluid,

$$f^b = U\left[(c_1^b + c_2^b y)\cosh(2\pi y/\ell) + (c_3^b + c_4^b y)\sinh(2\pi y/\ell)\right] \tag{28}$$

To facilitate the determination of the constants using the remaining boundary conditions, the following procedure will be applied. First, the continuity condition on the x-components at the fluid-fluid interface will be satisfied by requiring

$$v_x^a = v_x^b = U\sin(2\pi x/\ell) \tag{29}$$

The condition on the normal components at the fluid-fluid interface and the condition of no-slip and no normal flow at the electrode surface are applied next, to obtain a solution for the fluid motion in terms of U(the maximum

velocity at the fluid-fluid interface). The final condition on the total tangential shear stress is then used to couple the field and flow solutions by relating U to the potential amplitude V_o. The solution in terms of U is given by

$$\psi^a = Uy\, e^{-\alpha y/d} \sin(\alpha x/d) \tag{30}$$

and

$$\psi^b = U \frac{-\alpha(y+d)\sinh(\alpha y/d) + y \sinh\alpha \sinh[\alpha(1+y/d)]}{\sinh^2\alpha - \alpha^2} \sin \alpha x/d \tag{31}$$

where

$$\alpha = 2\pi d/\ell$$

Application of equation (23) obtains the velocity components in terms of U. Finally, equation (15) is used to relate the velocity U to the amplitude of the applied potential V_o ; substituting and rearranging terms yields

$$U = g(\alpha)\left(\frac{\pi \varepsilon_a}{4\ell\mu_b}\right)\left(1 - \frac{\sigma_a \varepsilon_b}{\varepsilon_a \sigma_b}\right)V_o^2 \tag{32}$$

where

$$g\left(\alpha, \frac{\sigma_a}{\sigma_b}, \frac{\mu_a}{\mu_b}\right) = (\sinh^2\alpha - \alpha^2)\Big/\left\{\left[2\frac{\mu_a}{\mu_b}(\sinh^2\alpha - \alpha^2) + \sinh 2\alpha - 2\alpha\right]\cdot \left[\cosh\frac{\alpha}{2} + \frac{\sigma_a}{\sigma_b}\sinh\frac{\alpha}{2}\right]^2\right\}$$

The form of this result is in agreement with the dimensional analysis which indicated for Re and Ry approaching zero that

$$U \longrightarrow S(0,0)\frac{\varepsilon}{\mu\ell} V_o^2 \tag{33}$$

Examination of this result for U shows that the sense of the steady state flow (i.e., the sign of U) is determined by the ratio of the

time constants which characterize the charge relaxation process in the two regions. The factor g is always positive, assuming the essentially positive nature of the fluid parameters. This fact is readily apparent when it is noted that the function $\sinh \alpha - \alpha$ is always positive for $\alpha > 0$. A sketch of this function for $2\frac{\mu_a}{\mu_b} = 0.2915$ and $\frac{\sigma_a}{\sigma_b} = 0.01515$ is shown in Figure 4. In the experiment, the depth d of the lower layer of fluid was chosen so the maximum value of this geometrical factor was attained; this in turn gives the maximum velocity at the interface for a given value of V_o. The stream lines for the flow are shown in Figure 5.

IV. Experiment and Results

The arrangement of an experiment to demonstrate the above theoretical explanation of the cellular flow is given in Figure 6. The fluids are contained within a pyrex tank attached to an insulating base which supports the electrode structure for the applied potential. The electrodes are electrically connected to a resistance bridge, which in turn is connected to the high voltage power supply as shown in Figure 6. An insulating top which supports a free electrode is used to approximate the boundary conditions (i.e., no-slip and vanishing field) at infinity. The electrode structure consists of equal area brass foil strips whose width and spacing were chosen to give a good fit to the continuum electrode of the theory and still not support arcing at the largest experimental voltages. The inner dimensions of the tank are 4.000 inches X 0.965 inches X 2.05 inches deep. The electrodes are 1.600 inches X 0.200 inches X 0.002 inches brass foil strips. The resistance bridge is constructed of 22 megohm resistors.

To observe the flow, a syringe was used to entrain small-diameter bubbles of air in the fluid. These small bubbles were then injected into the fluid in a plane along the center of the tank, and as near as possible to the fluid-fluid interface. The two fluids

used were Mazola corn oil and Dow Corning FS-1265 silicone oil. The properties of these fluids as used in the calculations are listed in Table 1. These two fluids are transparent, with the corn oil exhibiting a slight straw color, and the Dow Corning FS-1265 being colorless. In order to obtain the necessary flow data without creating a disturbance of the electric field, a photographic technique was used. Under intense illumination, the bubbles appeared as brighter points of light, and left distinct images on the film. Using a calibrated shutter and keeping the times of exposure short yielded accurate data for the determination of the magnitudes of the velocity at various points of the flow. The assumption of a two-dimensional flow was observed to be well satisfied in the central plane of the tank. Long time exposures were also obtained after a steady flow was reached; these films gave a good record of the actual streamlines of the flow.

As the bubbles dissipated, it was observed that the flow occurring in the tank remained unaffected; hence, it was concluded that the presence of even a large quantity of bubbles did not significantly distort the fluid motion. Two major disadvantages in using the bubbles were that they had, of necessity, to be renewed periodically; and, further, their motion due to the buoyancy force set the lower limit on the usable flow data which could be determined accurately. For the given experimental geometry and parameters, this lower boundary occurred at approximately V_o = 0.4kv, which corresponds to a maximum field intensity along the interface of $2.74(10^4)$v/m. The upper limit on the range of voltages used was an instability of the fluid-fluid interface which took the form of filaments of the Dow Corning FS-1265 erupting along the electric field lines in the regions of maximum field intensity. This instability occurred at approximately V_o = 8.1 kv, which corresponds

to a maximum field intensity along the interface of $5.46(10^5)\ \frac{V}{m}$.

The results of the experiment are presented in the form of a streak photograph which gives the streamlines of the observed flow and a plot of U versus V as measured compared with the model prediction of Eq. (32). In the experiment, as indicated in Figure 6, V is the peak-to-peak applied potential associated with the electrode structure and resistance bridge. To relate this voltage to the amplitude V_o of the theoretical model, it is assumed that V_o corresponds to the fundamental Fourier component of a triangular wave of amplitude V/2 and spatial period 2 . This assumption yields

$$V_o = (4/\pi^2)\ V \tag{34}$$

and for the data of Table 1, equation (32) becomes

$$U = 0.045\ V^2 \tag{35}$$

where U is in millimeters per second and V is in kilovolts. The streak photograph is shown in Figure 7, and the U vs V plots are given in Figure 8.

V. Conclusions

In comparing the actual flow streamlines with those predicted by the theoretical model as shown in Figure 5, it is seen that the general form including the sense of the flow agrees well; but there are some differences. In particular, the actual surface is slightly deformed and the presence of the end walls and tank top has caused the cell appearance to differ from that seen in Figure 5. The agreement between the measured values of U and those predicted by Eq. (32)(the curve marked theoretical with $V_o = 4V/\pi^2$) is good; the parabolic dependence with V is very evident, and the fact that the experimental curve falls below the theoretical curve may be explained by consideration of the finite extent of the fluid (i.e.,

the effects of tank walls) and by examination of the Reynolds' numbers. The electric Reynolds' number Re for both fluids satisfied the condition $Re < 1$; for a velocity of U = 1 millimeters per second and $\ell = 3.4(10^{-2})$ meters

$$R_e^a = 1.6\ (10^{-2}) \quad \text{, corn oil}$$

and

$$R_e^b = 5.5\ (10^{-4}) \quad \text{, silicone oil}$$

For the ordinary Reynolds' number Ry and the same characteristic values

$$R_y^a = 0.57 \quad \text{, corn oil}$$

and

$$R_y^b = 0.13 \quad \text{, silicone oil}$$

In the corn oil, the ordinary Reynolds' number is equal to unity for a velocity 1.7 mm/s, and the experimental data begins to deviate significantly when U > 2mm/s. This implies that the convective inertial term $\rho\bar{v}\cdot\nabla\bar{v}$ is becoming important in the flow; further, the fact that even at values of $R_y^a > 1$ there is agreement is not unusual, as this is also the case for Stokes' and Oseen's solutions for the problem of the sphere.[15] In general, the theoretical model is successful in predicting the flow in the range for which $Re < 1$ and $Ry < 1$, and appears to yield a reasonable explanation for the observed continuum electromechanical interaction present in the experiment.

Acknowledgments:

The authors wish to thank Sir Geoffrey Taylor for discussion concerned with the related flow problem found in the "Taylor pump". This work was supported under NASA grant No. NsG-368.

FLUID PARAMETER	DOW CORNING FS-1265	MAZOLA CORN OIL
Dielectric constant, ϵ/ϵ_0	6.95	3.1
Conductivity, σ $(\Omega\,m)^{-1}$	3.3 (10^{-9})	0.5 (10^{-10})
Specific gravity	1.25	0.91
Kinematic viscosity, ν (cs.)	300	60
Absolute viscosity, μ $kg(ms)^{-1}$	0.375	0.0546

Table 1. Nominal room temperature (20-25°C) fluid properties used in the theoretical calculations.

REFERENCES

1. Taylor, G. I., and McEwan, A. D., J. Fluid Mech., 22, 1, (1965).
2. Melcher, J. R., Field-Coupled Surface Waves, (M.I.T. Press, Cambridge, Massachusetts, 1963).
3. Malkus, W. V. R., and Veronis, G., The Physics of Fluids, 4, 13, (1961).
4. Reynolds, J. M., The Physics of Fluids, 8, 161, (1965).
5. Analogous deformations have been observed on the interface of a magnetic fluid stressed by a perpendicular magnetic field. For pictures of these "spikes", see Rosensweig, R. E., Science and Technology, July, (1966).
6. These pictures are taken from the film Complex Waves II, by J. R. Melcher, produced by Educational Development Center, Inc., Newton, Mass., for the National Committee on Electrical Engineering Films.
7. Taylor, Sir Geoffrey, Proc. Royal Society, A, 291, 159 (1966).
8. Chandrasekhar, S., Hydrodynamic and Hydromagnetic Stability, (Clarendon Press, Oxford, England, 1961), p. 44.
9. Melcher, J. R., The Physics of Fluids, 9, 1548 (1966).
10. Stratton, J. A., Electromagnetic Theory, (McGraw-Hill Book Company, Inc., New York, 1941), pp. 137-140.
11. Fano, R. M., Chu, L. J., and Adler, R. B., Electromagnetic Fields, Energy and Forces (John Wiley and Sons, Inc., New York, 1960) pp. 84-86.
12. Stuetzer, O. M., The Physics of Fluids, 5, 534, (1962).
13. Bridgman, P. W., Dimensional Analysis, (Yale University Press, New Haven, Connecticut, 1963) p. 36.
14. Prandtl, L., and Tietjens, O. G., Fundamentals of Hydro- and Aeromechanics, (Dover Publications Inc., New York, 1957), p. 262.
15. Schlichting, H., Boundary Layer Theory, (McGraw-Hill Book Co., Inc., New York, 1960) pp. 95-98.

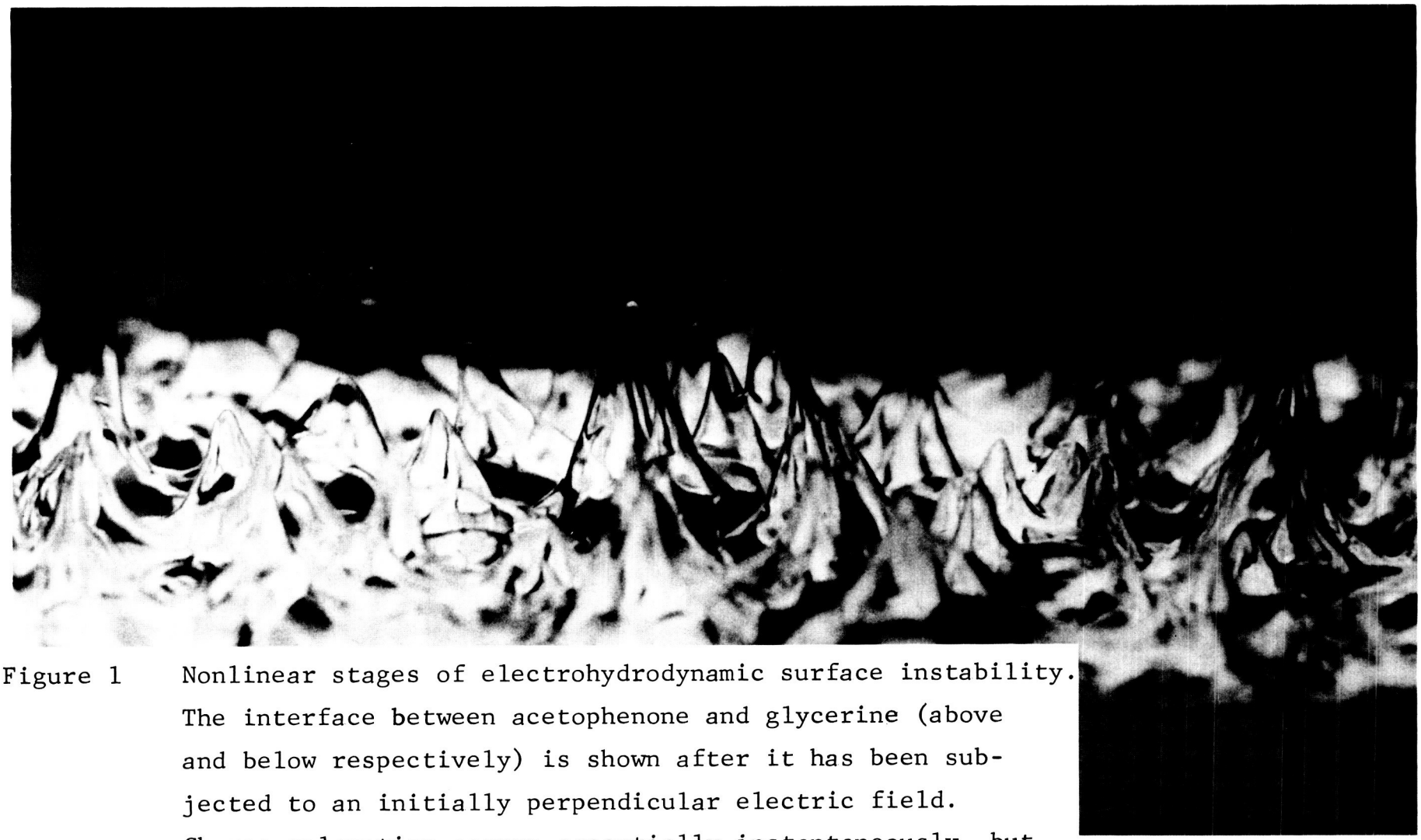

Figure 1 Nonlinear stages of electrohydrodynamic surface instability. The interface between acetophenone and glycerine (above and below respectively) is shown after it has been subjected to an initially perpendicular electric field. Charge relaxation occurs essentially instantaneously, but

a

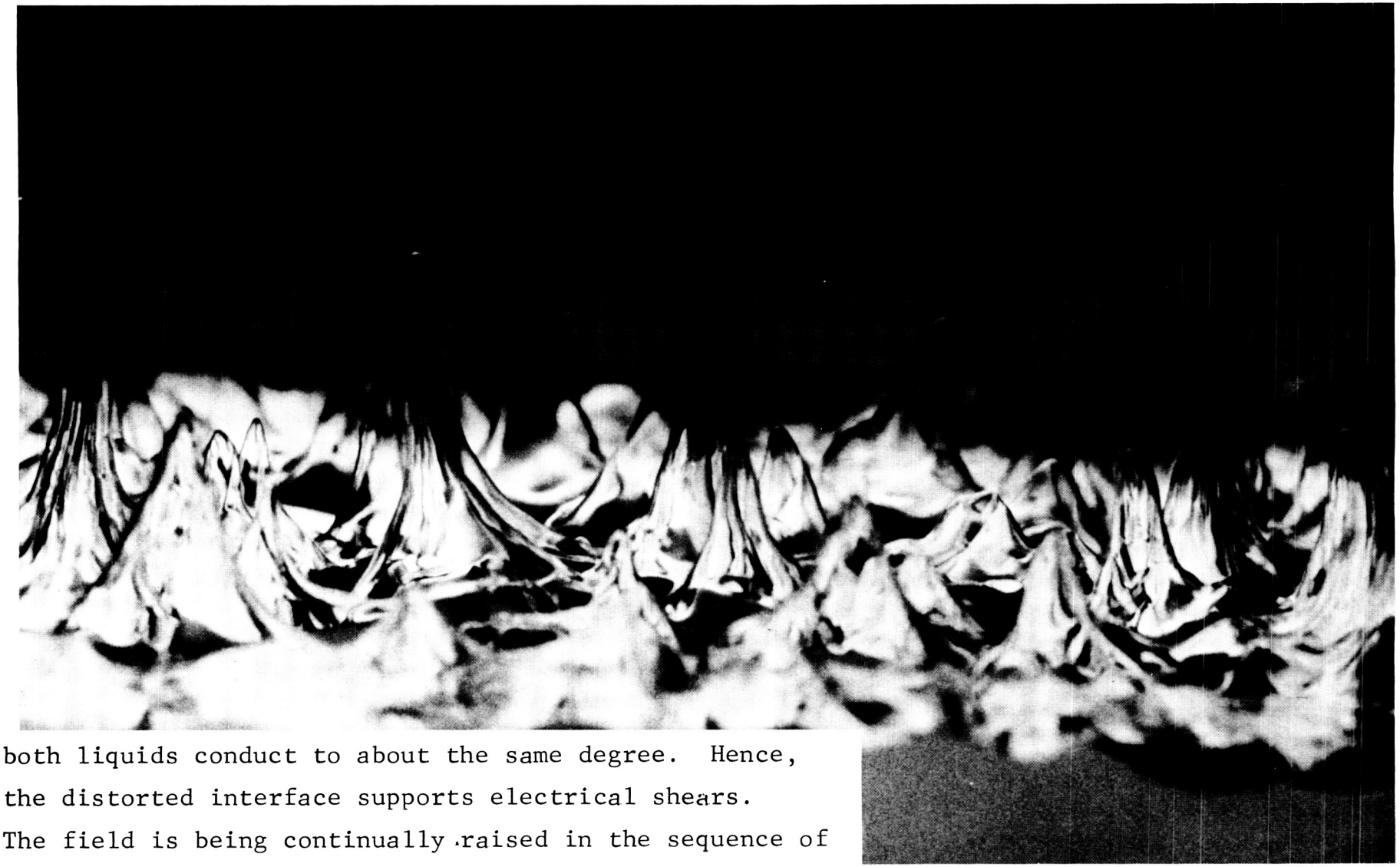

both liquids conduct to about the same degree. Hence, the distorted interface supports electrical shears. The field is being continually raised in the sequence of pictures. At constant electric field, the deformations remain bounded in amplitude.

b

C

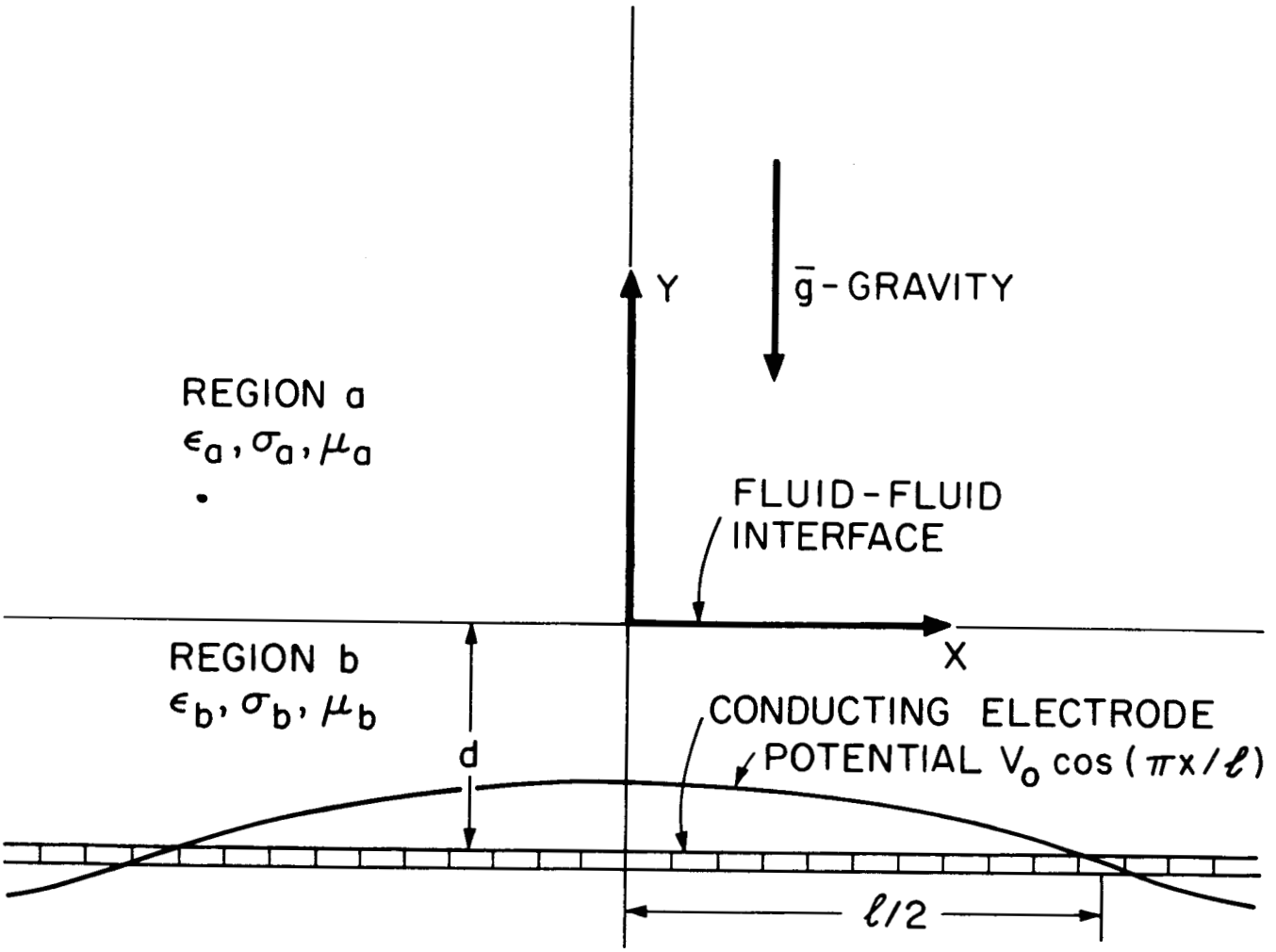

Figure 2 Cross-sectional view indicating the fluid-fluid interface and the conducting electrode. The electrode is in electrical contact with the fluid in the region below the interface.

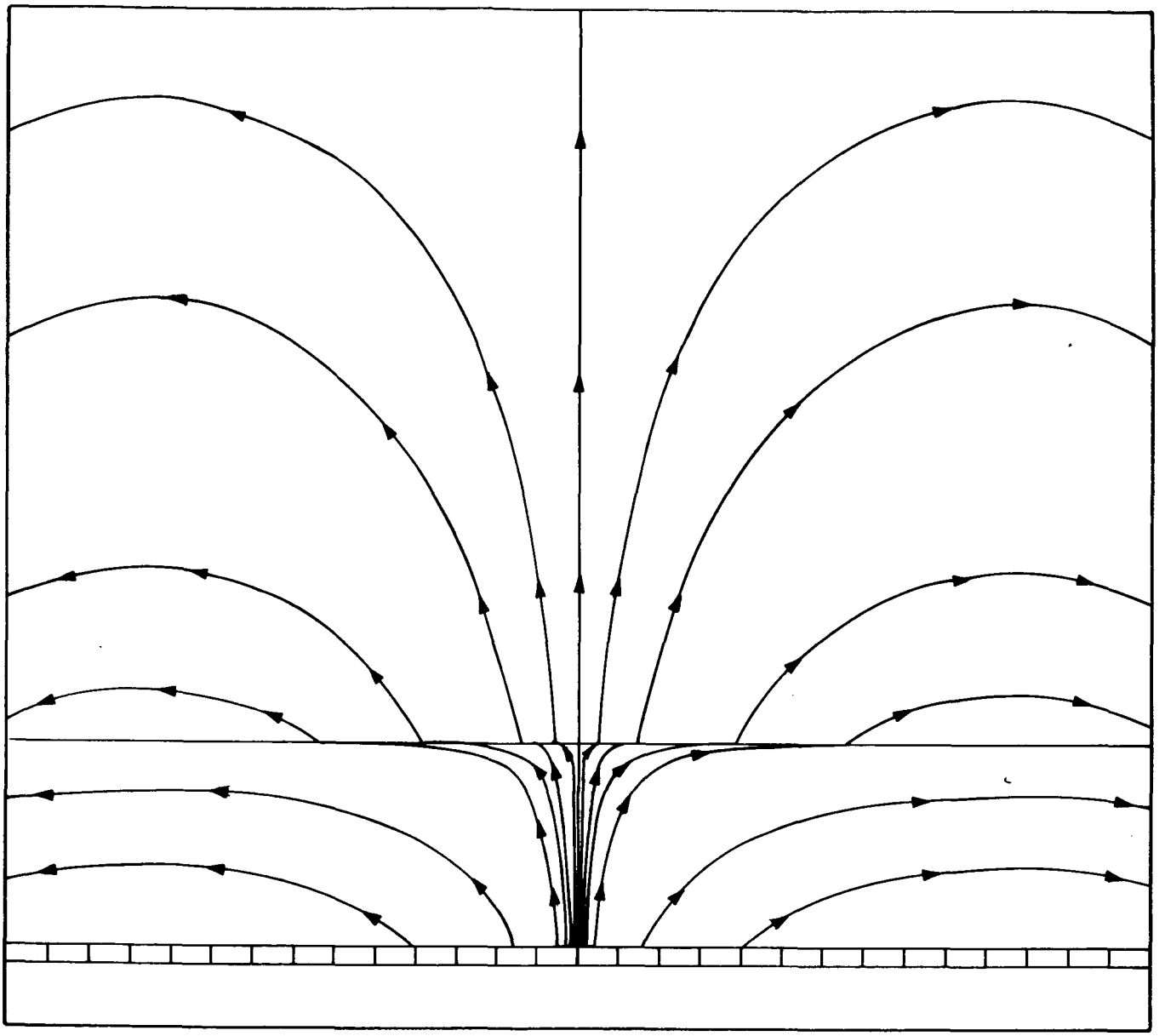

Figure 3 Cross-sectional view showing the lines of force for the electric field. It should be noted that the field lines shown were chosen to indicate clearly the refraction through the fluid-fluid interface; as a consequence, the density of the field lines in any portion of the diagram does not relate to the field intensity in the usual way.

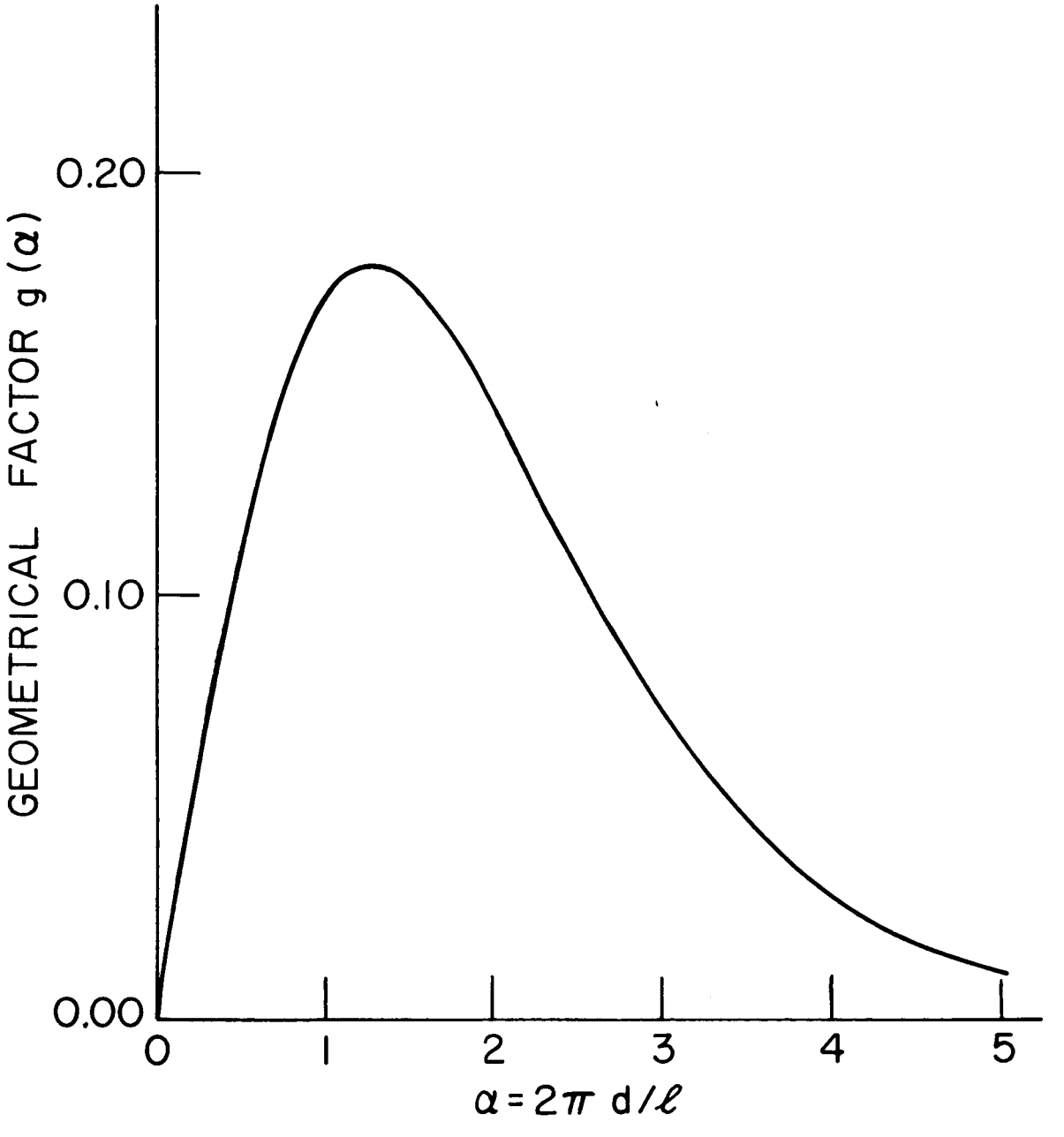

Figure 4 A plot of the geometrical factor $g(\alpha)$ versus α for the specific values $2\mu_a/\mu_b = 0.2915$ and $\sigma_a/\sigma_b = 0.01515$.

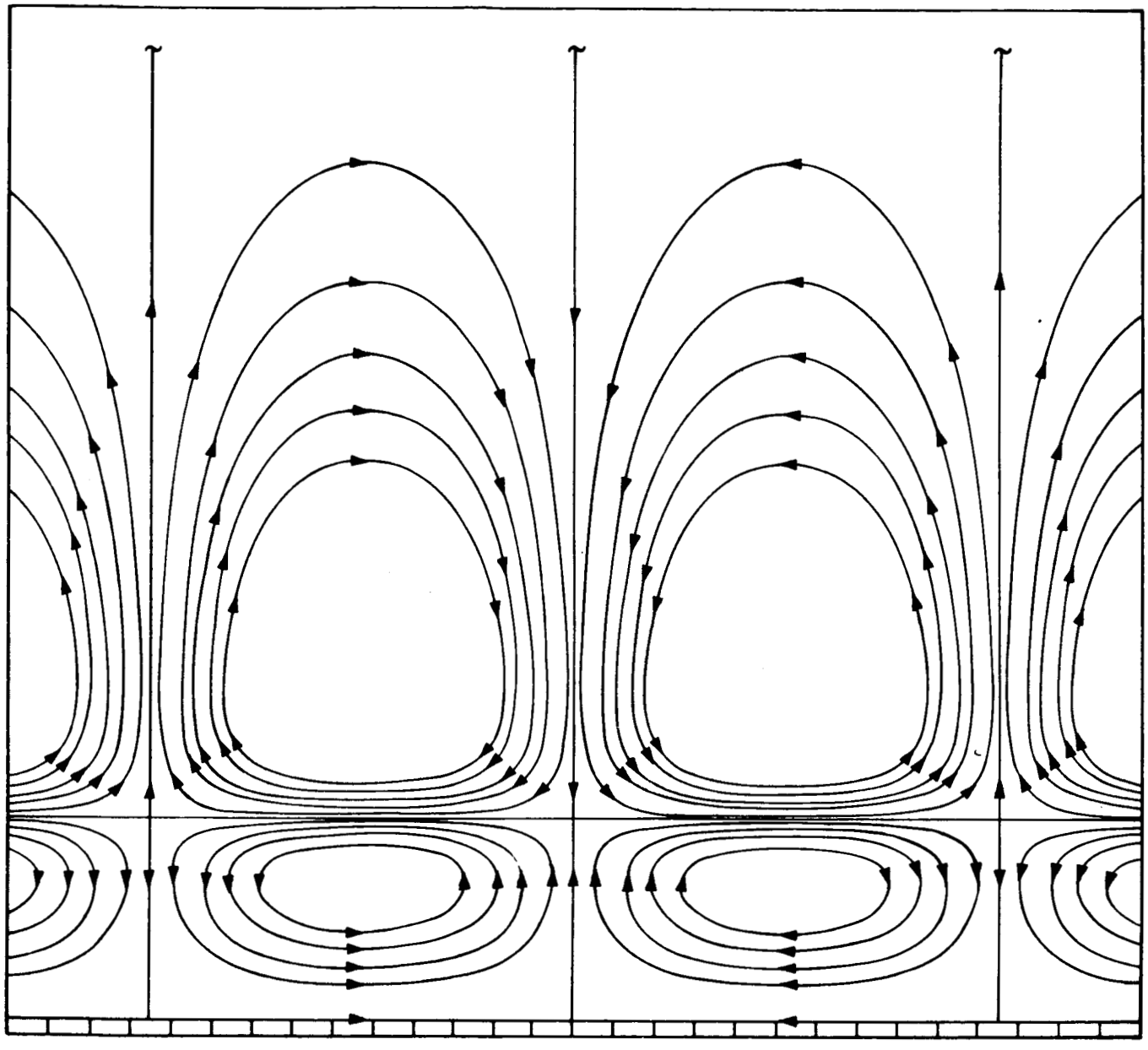

Figure 5 Streamlines of the flow for $\alpha = 1.67$, $2\mu_a/\mu_b = 0.2915$ and $\sigma_a/\sigma_b = 0.01515$. The streamfunction is normalized to unity at the vortex axis in the upper cells.

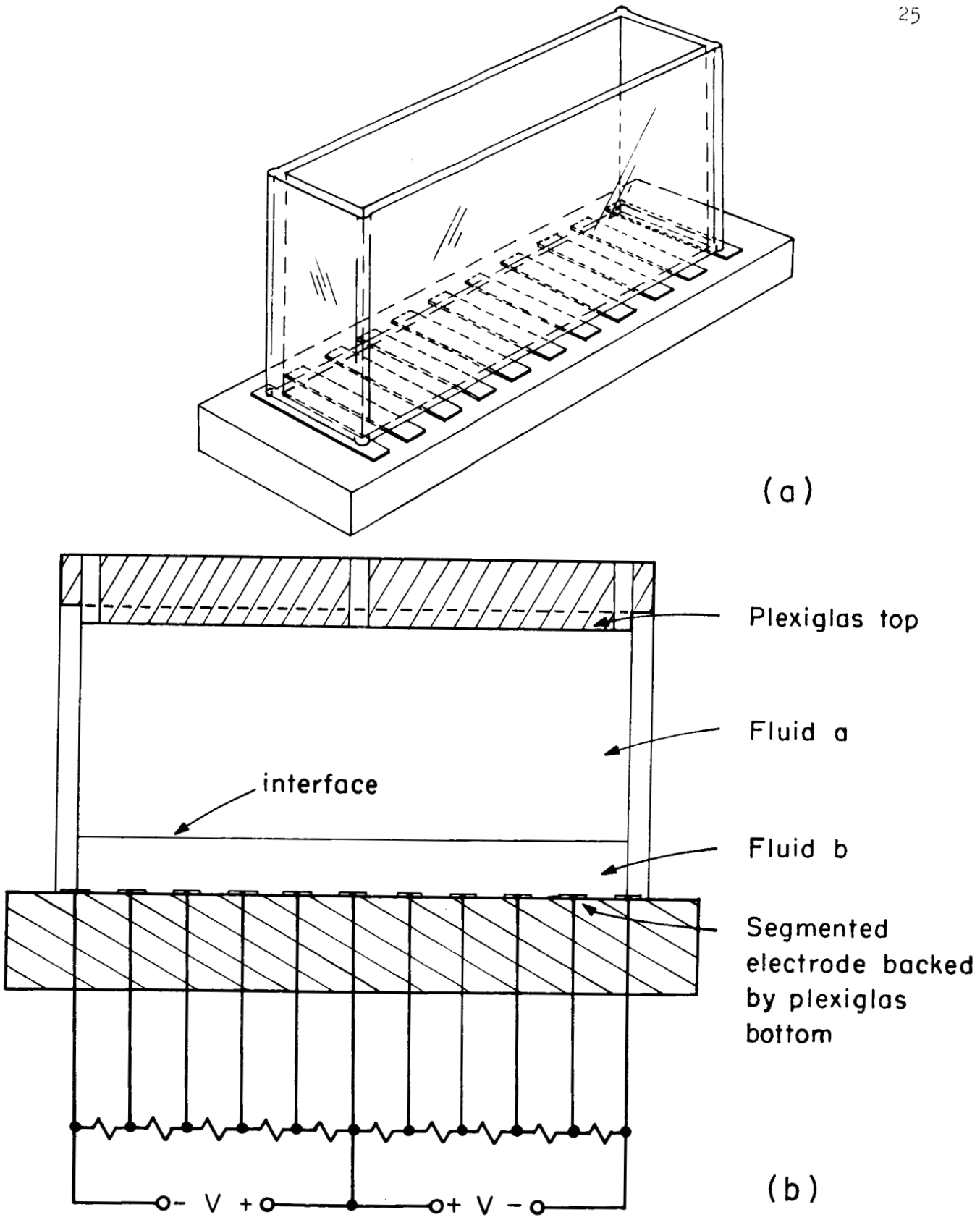

Figure 6 a) Schematic diagram of experimental tank.

b) Side view of tank, showing connection of electrodes and resistance bridge to power supply. The relative location of the fluid-fluid interface above the electrodes and insulating base is indicated in the cross-section.

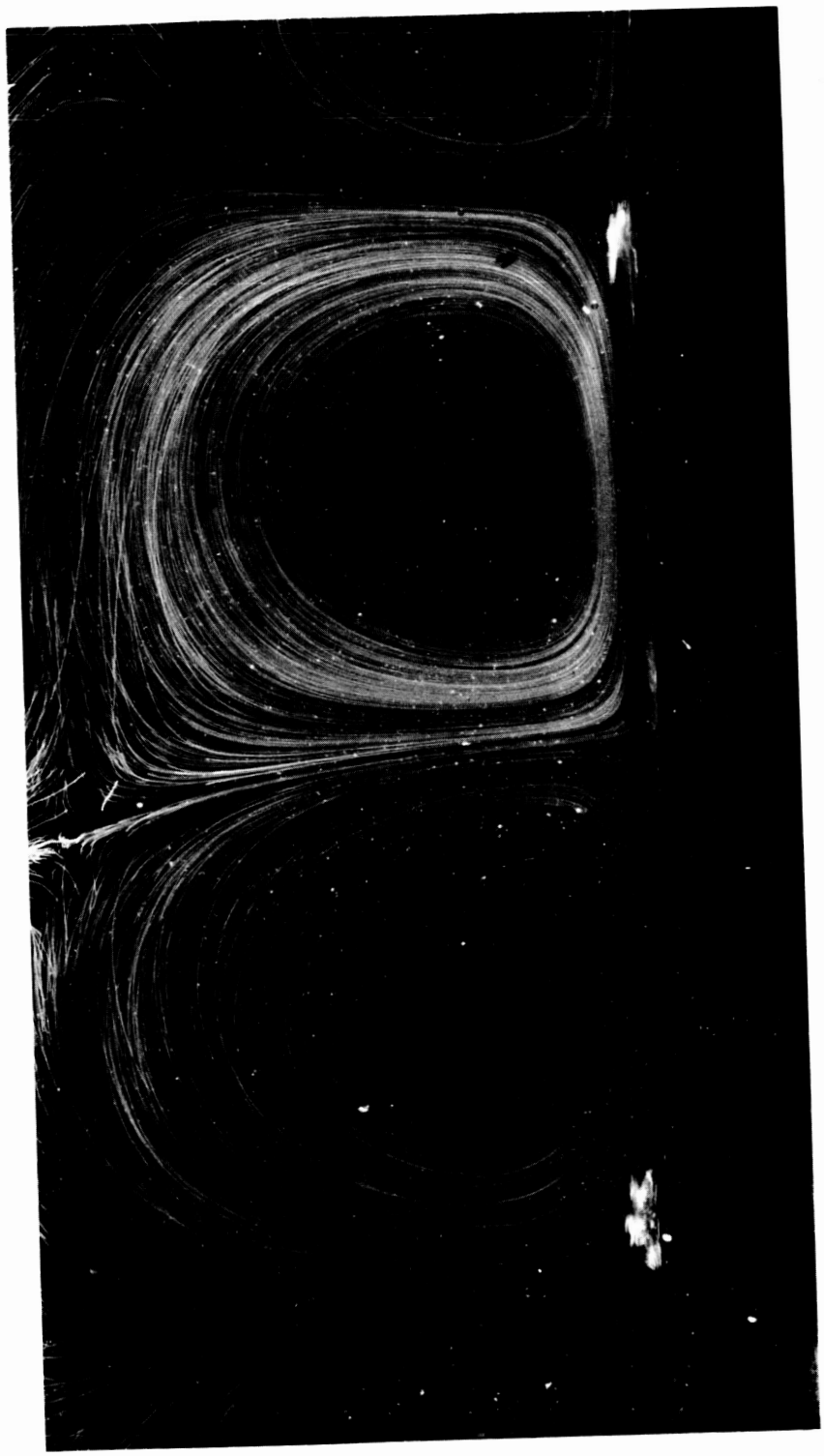

Figure 7 Streak photograph indicating the streamlines of the induced flow in the experimental tank.

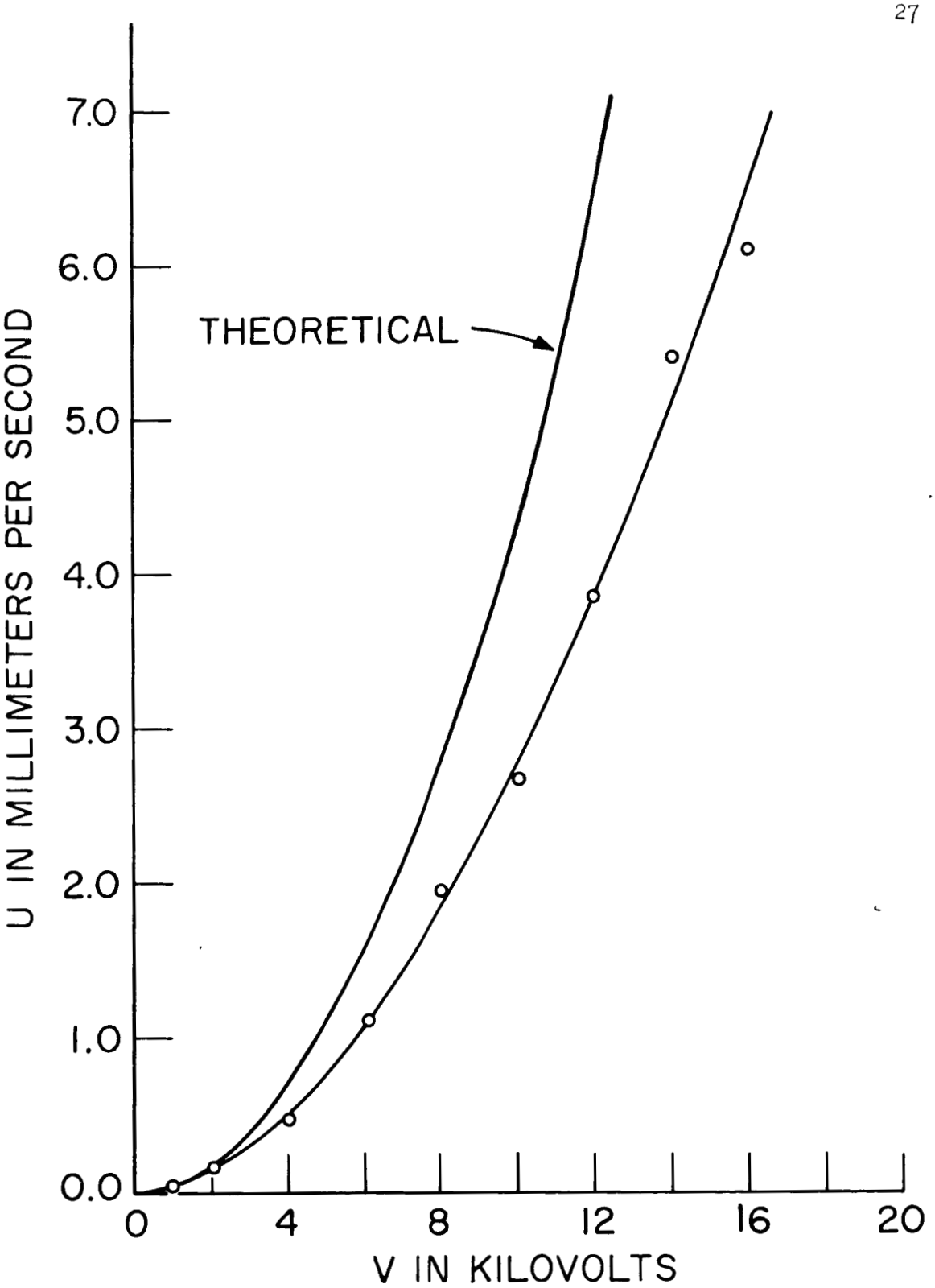

Figure 8 Plot showing U in millimeters per second versus V in kilovolts for the experiment using Mazola corn oil and Dow Corning FS-1265 silicone oil. The curve marked 'theoretical' is from Eq. (32) with $V_0 = {}^{4v}/_{\pi^2}$ and the fluid paparmeters of Table 1.